Supplementary Information

Supplementary Figures:

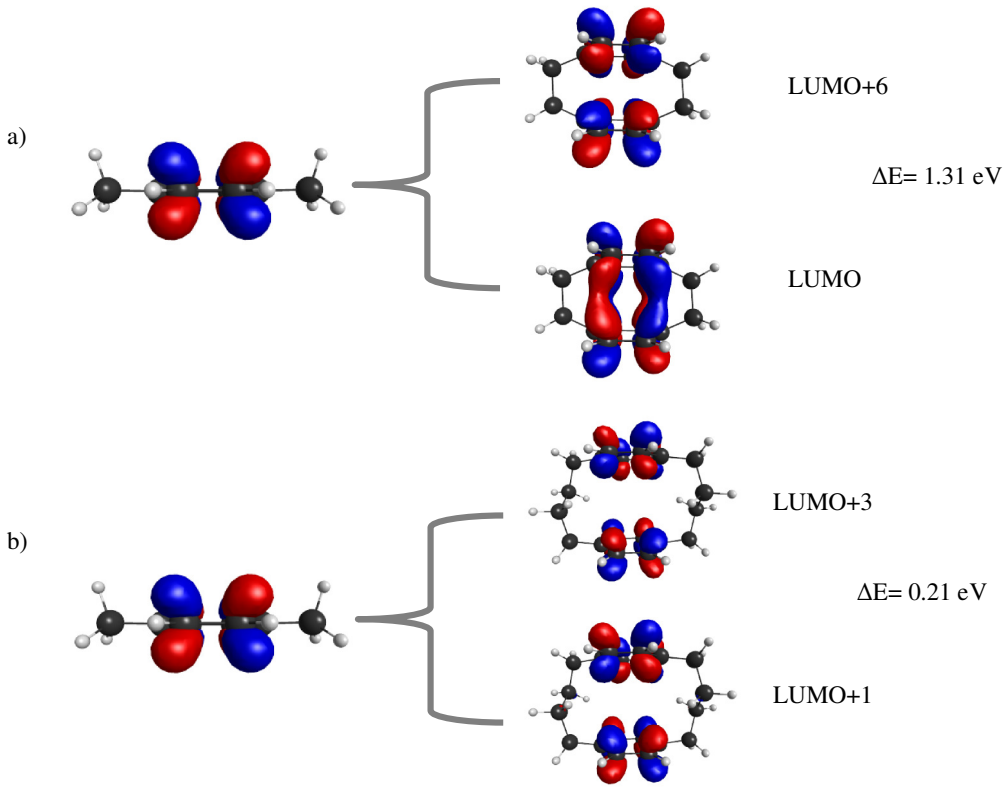

Supplementary Figure S1: ***Calculation Results:*** *Bonding and Antibonding combinations of the xylene LUMO in a) [2,2]paracyclophane and b) [4,4]paracyclophane*

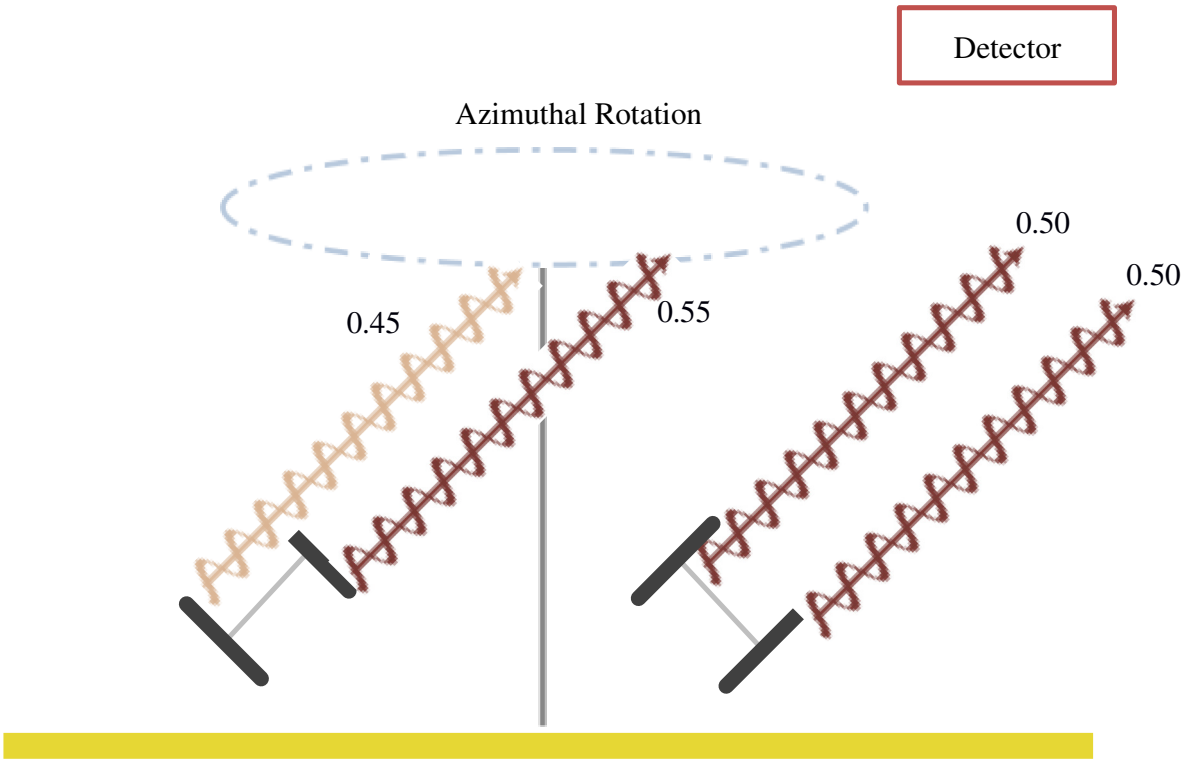

Supplementary Figure S2: Effect of Azimuthal orientation on shadowing. The molecular orientation on the right corresponds to no shadowing, and thus equal contribution of top and bottom rings (0.5) to total intensity (1.0). The molecule on the left shows the case of maximum shadowing of the bottom ring, resulting in a higher contribution from the top ring (0.55) than the bottom (0.45).

Supplementary Methods:

Calculation Details: Molecules were structurally relaxed by performing spin-unrestricted calculations using the B3LYP exchange-correlation functional and LACV3P** basis set using the Q-Chem software suite[47]. Default grids and convergence thresholds were used for relaxation. Subsequently, single-point calculations were carried out using B3LYP/LACV3P**++ to calculate molecular energy levels. Binding energies were calculated for both molecules with an Au-dimer, following the procedure outlined by Schneebeli, et al. [7].

For NEXAFS Simulations and orbital isosurfaces of Carbon K-edge excited molecules, GPAW, a grid-based real-space projector-augmented-wave (PAW) code was employed with the B3LYP exchange-correlation functional[48]. Isolated molecules were first relaxed to their optimized geometries, before conducting single point calculations. Default grid spacings and convergence thresholds were employed. All NEXAFS calculations were performed using the half-core-hole approximation[38].

RPES analysis procedure: For resonant photoemission (RPES) measurements, the incident photon energy was scanned across the carbon 1s absorption edge with a photon energy step of 0.1 eV. For each photon energy, a 90 eV photoemission spectrum was measured. This measurement window contained the whole valence band spectrum as well as the Au $4f_{5/2}$ and Au $4f_{7/2}$ peaks which served to calibrate the binding energy. During this measurement, the electron current due to X-ray absorption on the last mirror of the beamline optical system was measured. This current signal was used for initial photon energy calibration and intensity normalization. The measurements were performed in magic angle conditions, i.e. the polarization as well as the electron analyzer were at 54.7° with respect to the sample normal, thus yielding a signal independent of the molecular orientation on the sample.

The RPES spectra were first normalized to the separately measured absorption on a clean Au(111) substrate. Next, all valence band (VB) scans were aligned using the Au 4f photoemission peaks, which yielded the final correction to the photon energy calibration. The binding energy of the Au $4f_{7/2}$ peaks in each scan was set to 84 eV. For both types of films, monolayer and multilayer, we used the second-order light C1s peak in RPES to perform a further correction for any charging effects. The non-resonant signal was measured in the pre-edge region at $h\nu$=283 eV and subtracted from each scan in the 2D RPES map.

To separate the different core-hole decay channels, we first measured the normal Auger

peak shape at higher photon energy far above the edge at hν=310 eV. The subtraction of the Auger peak signal was done in the kinetic energy scale. For each photon energy, the intensity (multiplicative factor) and possible spectator shift of the Auger peak was assessed. With a best fit procedure, the Auger peak intensity and energy shift due to spectator electron was obtained, and was further subtracted from the spectra to leave only the resonant photoemission intensity (participator intensity). The intensity of the subtracted Auger signal closely resembles the NEXAFS intensity throughout the absorption edge, and spectator energy shifts of the order of 2-4 eV were found for photon energies between 284-288 eV (i.e below the ionization edge). This non-resonant and Auger subtraction procedure was employed to the monolayer as well as multilayer RPES data. The intensity of the RPES was further normalized to the overall intensity (Auger + participator).

The core hole clock method was then used to determine the charge transfer times in monolayer systems. In a well-coupled molecule-metal system, charge transfer (CT) to the substrate suppresses the resonant photoemission signal. The intensity of the suppressed signal, obtained from the RPES map is then compared to the reference multilayer signal intensity where we assume no CT channel is available, i.e. the RPES signal is unquenched. Before measuring the quenching of the RPES signal, the monolayer data has to be normalized to the multilayer (for the coverage, photon illumination due to absorption etc.). Here we assume that, for each photon energy scan, the probability of core-hole decay should be 1. This means that the sum of all decay channels (i.e. total integrated intensity) should be equal for both mono- and multilayer systems. The charge transfer time is then determined using Equation 1 in the main text.

Charge-transfer model: We measure the CT dynamics from the LUMO, which is, according to our DFT ground state calculations, distributed across the benzene rings of both molecules. The probability to create a core-hole on either ring is thus equal to 1/2. It is however important to note that the signal coming from the lower ring is shadowed by the upper ring due to inelastic electron scattering. We use the measured attenuation of the Au 4f electrons that pass through the entire paracyclophane monolayer as a reference and scale it by half of the layer thickness to obtain the signal attenuation from the inner ring[49]. We find for the Au 4f peak an attenuation of ~ 35% in a monolayer, which yields an attenuation of ~20% for the signal coming from the lower ring. We further note that our electron detector is placed at 54° from the surface normal, and that the paracyclophane molecules adsorb with a tilt angle of 45° evenly around the surface normal. This indicates that not all paracyclophane molecules adopt a geometry in which the upper ring attenuates the signal from the lower ring.

Supplementary Figure S2 illustrates two extreme orientations where the shadowing effects are either zero or maximal. The orientation shown on the left results in a maximal intensity difference due to shadowing with I_{upper} = 0.55 and I_{lower} = 0.45) while the one on the right has equal contribution from both rings with $I_{upper} = I_{lower} = 0.5$. In this latter case we consider that regardless of the azimuthal orientation, the entire molecular film thickness d equally attenuates the Au signal beneath ($\exp(-d/\lambda) = 0.65$, λ being the elastic mean free path of electrons[49]). Therefore, the signal from the molecules in the right hand side of Figure S1 is thus equally attenuated by $\exp(-d/2\lambda) = 0.8$ for both, lower and upper ring. By averaging over all molecular orientations, the ratio of the signal from the upper and lower rings is 0.525:0.475. We use these attenuation ratios in our core-hole clock analysis (Eqs. 3-5 in the main text).

Error estimates for CT times have been obtained from the intensity uncertainties of the $\delta\langle q_{22}\rangle = 0.02$ and $\delta\langle q_{44}\rangle = 0.02$ and by using these in Eqs. 3-5 to determine the spreads of the CT time values throughout the considered range ($0 < q_{lower} < 0.085$, this upper limit is set by the $\tau_{lower} < \tau_{22}$ constraint). For $\tau_{44,}$ the resolution of the CHC method is much poorer[23] and the reported value should serve as a lower bound.

Supplementary References

47. Shao, Y. *et al.*, Advances in methods and algorithms in a modern quantum chemistry program package. *Physical Chemistry Chemical Physics* 8 (27) (2006).

48. Mortensen, J.J., Hansen, L.B., & Jacobsen, K.W., Real-space grid implementation of the projector augmented wave method. *Physical Review B* 71 (3), 035109 (2005).

49. Cumpson, P.J. & Seah, M.P., Elastic Scattering Corrections in AES and XPS. II. Estimating Attenuation Lengths and Conditions Required for their Valid Use in Overlayer/Substrate Experiments. *Surface and Interface Analysis* 25 (6), 430-446 (1997).